한국에너지공학회지(2002), 제11권 제3호
Energy Engg. J(2002), Vol. 11, No. 3, pp. 254~261

Characteristics of the Multi-kW Class Polymer Electrolyte Membrane Fuel Cell Stack for a Hybrid Electric Golf Cart

I.-H. Oh, S.-J. Shin, J.-H. Jo, S.K. Park, H.Y. Ha, S.-A. Hong, S.-Y. Ahn*, Y-C. Lee*, S.-A. Cho, J.-B. Ju** and T.W. Lim*****

Fuel Cell Research Center, Korea Institute of Science and Technology
**Department of Chemical Engineering, Sungkyunkwan University*
***Department of Chemical Engineering, Hongik University*
****Fuel Cell Vehicle Team, Hyundai Motor Company*

Abstract — The fabrication method for the main components of the polymer electrolyte membrane fuel cell stack such as electrodes, membrane-electrode assemblies, and bipolar plates was established for the effective electrode area of 240 cm^2. A counter-flow type 100-cell stack was fabricated by using the above components and then a maximum power of 7.44 kW for H_2/O_2 and 5.56 kW for H_2/air could be obtained at 70°C and 1 atm. It was seen that the distribution of the OCV for unit cells in the stack was uniform but the voltage deviation increased as the load increased due to the IR drop and the electrode polarization. The stack was applied to the power source of the fuel cell/battery hybrid electric golf car. It produced about 1 kW at a room temperature operation during the test run, which occupied about 43% of the total power required by the 2.3 kW motor.

1. Introduction

Polymer electrolyte membrane fuel cell (PEMFC) is an adequate system for the power source of the zero-emission vehicles, as its power density is higher compared to other types of fuel cell, the stack structure is rather simple, and there is no leakage or loss of electrolytes during the operation. It has also advantages of rapid start-up and response, long endurance, and flexibility of fuel usage from pure hydrogen to methanol and natural gas[1][2]. Particularly, Daimler-Chrysler, Ford, and Ballard Power Systems have established a consortium to produce fuel cell vehicles commercially 40,000 units per year by 2004. Therefore, the zero-emission vehicles driven by PEMFC are likely to be realized very soon[3].

In Korea, the prototype of 25 kW class fuel cell vehicle (FCV) is scheduled to be developed by 2002 according to the national program for next generation vehicles which was started in late 1998. The role of Fuel Cell Research Center of KIST in this program is to establish the fundamental technology of the high efficiency PEMFC stacks. Therefore, the fabrication method for the main components such as electrodes and membrane-electrode assembly (MEA), and the technologies for bipolar plates, gas sealing, and water and heat management have been established for single cells and short stacks[4]-[8]. The 5 kW class 100-cell stack has been also assembled and successfully applied to the power source of the fuel cell/battery hybrid golf cart[9][10]. Since there have been few papers that described the detailed fabrication procedure and the characteristics of the stacks, some aspects of the component preparation and the operating behavior of the PEMFC stack as well as the application of the stack to a hybrid electric golf cart were investigated in this work.

2. Experimental

The key component for the PEMFC stack is MEA and the fabrication procedure of the MEA is shown in Fig. 1. Pt/C powders (E-TEK) in which 40% of Pt were impregnated on carbon black supports were used as a catalyst for electrochemical reactions. The ink for the catalytic layers was prepared from the above Pt/C powders and Nafion solution which were suspended in n-butyl acetate (NBA) solvent, and then sprayed by screen printing over the carbon papers which had a carbon layer in advance to produce the

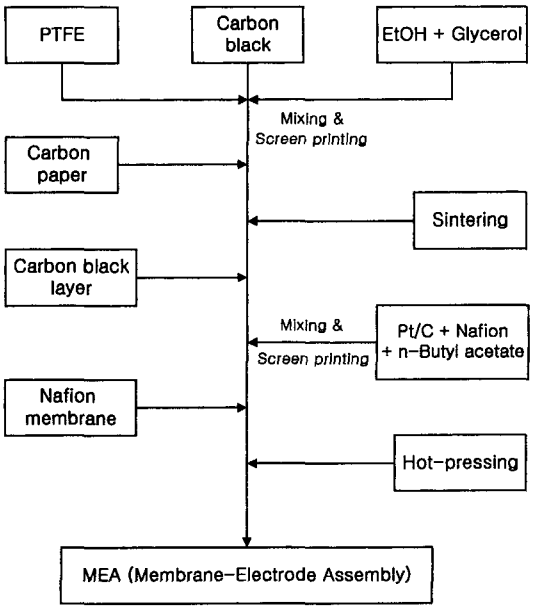

Fig. 1. Fabrication procedure of the membrane-electrode assembly.

electrodes. The Pt loading amounts were 0.4 and 0.7 mg/cm^2 for anode and cathode, respectively. The MEA was prepared by placing the above electrodes at the both sides of the pre-treated Nafion 115 membrane, followed by hot pressing at 140°C and 200 atm for 2 minutes. The electrodes of 25 and 200 cm^2 have been fabricated. The performance of the components was evaluated by measuring the i-V characteristics using single cells and the results were used for the fabrication of the 100-cell stack with the effective electrode area of 240 cm^2.

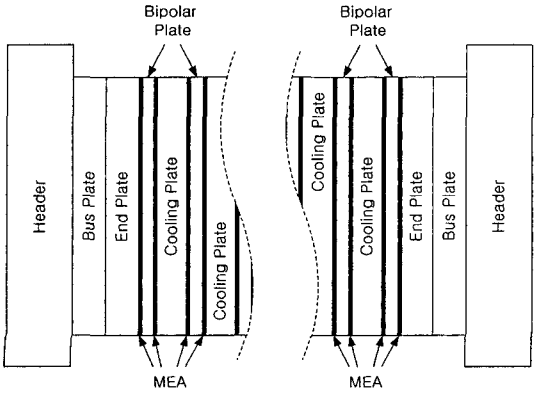

Fig. 2. Schematic diagram of the multi-kw class stack.

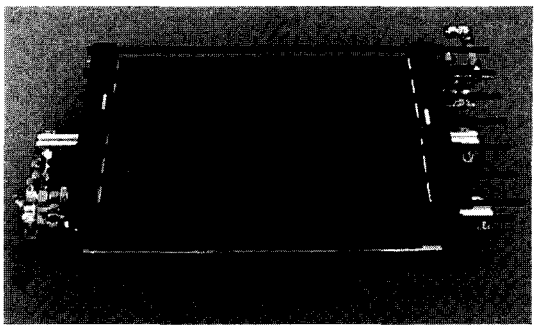

Fig. 3. Photograph of the 100-cell stack.

Figure 2 shows the schematic diagram of the 100-cell stack, which mainly consisted of the repeated units of MEAs and bipolar plates. Cooling plates are the bipolar plates that contains the cooling water channel inside, and therefore, MEA was placed between a bipolar plate and a cooling plate in this work. The heat produced during the operation was removed by flowing coolant. Bipolar and cooling plates, all made of graphite, had the serpentine type hydrogen flow field on one side and oxygen (or air) flow field on the other side. The flow direction of the oxidant and the fuel gas was opposite, and thus, the flow pattern was the counter-flow type. The flow fields and the gas manifolds were sealed by the pre-patterned gasket. Two pieces of the gold-coated bus plates, which were located at the both ends of the stack, collected currents from the stack and produced electricity to the outside. Headers, equipped with the inlets and outlets for hydrogen, oxygen (or air), and cooling water, were placed at two outermost ends of the stack. Several tie rods were used to tighten all of these components.

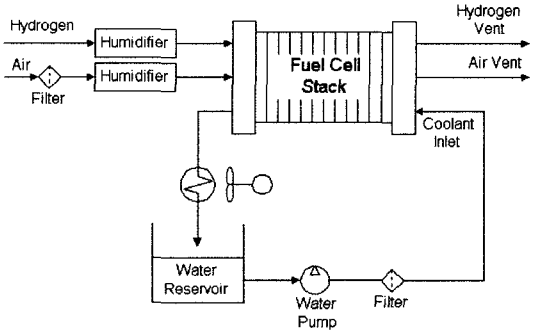

Fig. 4. Schematic diagram of the operating system for the multi-kW class PEMFC stack.

The photograph of the assembled 100-cell stack is shown in Fig. 3.

The stack was operated and evaluated by an operating system at 70°C and 1 atm, of which schematic diagram is represented in Fig. 4. Oxidant and fuel gases were humidified by using the bubble-type humidifier. After evaluation of the stack, it was applied to the power source of the fuel cell/battery hybrid golf cart and the change of the stack performance during the vehicle run was studied.

3. Results and Discussion

Figure 5 shows the size effect of the electrode area. Single cells with an effective electrode area of 25 cm^2 showed a current density of 928 mA/cm^2 at 0.6 V and at the given operating conditions using H_2 and O_2, with a power density of about 0.56 W/cm^2. When the electrode area increased to 240 cm^2, the cell performance decreased down to 500 mA/cm^2 at 0.6 V, namely 0.3 W/cm^2, due to the scale up problems. The decrease in cell performance at larger electrode is because there might occur non-uniform distribution of concentration, temperature and holding pressure inside the cell as the electrode area increases. The accumulation of water produced at the cathode side gas channel might result in the dead space for the gas diffusion to the cathode, and thus decrease the electrochemical reaction area. Stacking of such single cells into the 100-cell stack

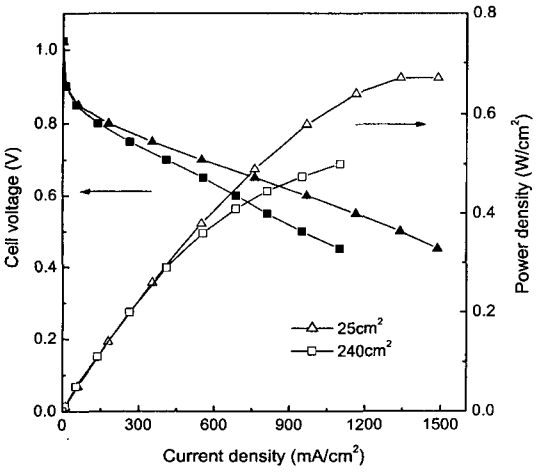

Fig. 5. Effect of the electrode area on the cell performance for a single cell.

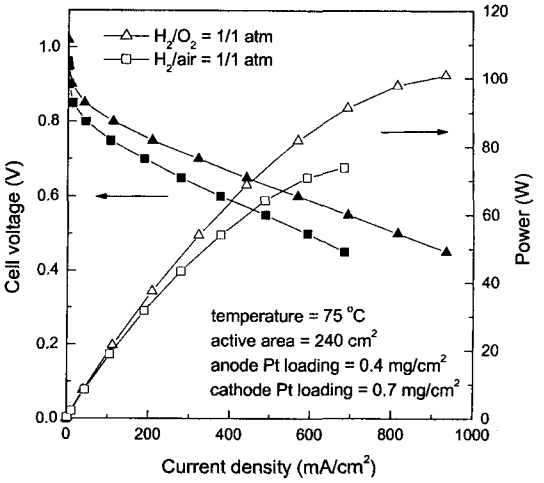

Fig. 6. Effect of the oxidants on the cell performance for a 240 cm^2 single cell.

results in the further decrease in the cell performance due to the non-uniformity between unit cells in the stack.

The polarization curves of the single cell with the effective electrode area of 240 cm^2 using the different oxidants of oxygen and air are shown in Fig. 6. The cell performance in the case of air is usually lower than that in the case of pure oxygen, because the partial pressure of oxygen in air is approximately 0.2 atm under atmospheric pressure. Oxygen gain is the amount of voltage drop of the cell when the oxidant is changed from pure oxygen to air with the same oxygen molarity. Oxygen gain depends on the structure or properties of the electrode, and particularly the amount of the voltage drop becomes significant at the higher current density region where the mass transfer in the gas phase is critical[11]. Therefore, oxygen gain is regarded as an index of the mass transfer resistance of oxygen in the cathode. From Fig. 6, it is seen that the degree of the voltage drop at the higher current density region was about 30%, which was smaller than the reported value of 40%[11]. Therefore, it seems that the electrodes fabricated by screen-printing were quite good for the air operation purpose. The maximum power of the single cell was 100 W at 0.45 V (900 mA/cm^2) for oxygen and 70 W at 0.45 V (650 mA/cm^2) for air. The designed output power of the 100-cell stack is, therefore, 10 kW for oxygen and 7 kW for air.

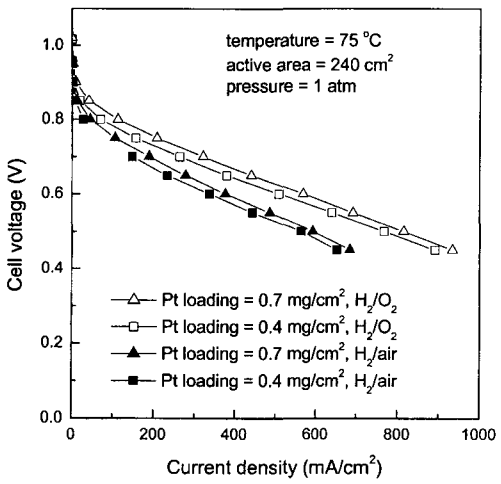

Fig. 7. Effect of the catalyst loading amount at the cathode on the cell performance for a 240 cm² single cell.

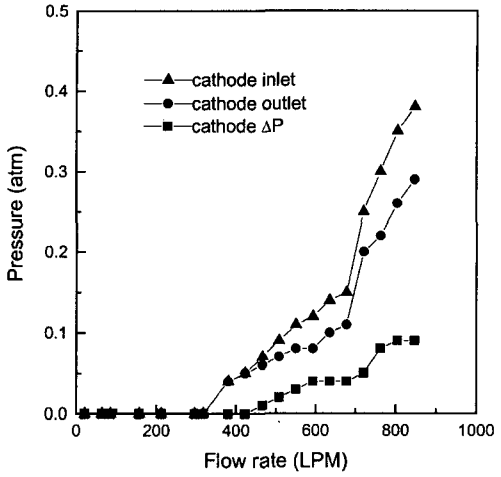

Fig. 8. Pressure drop of the 100-cell stack.

In general, the cell performance is almost linearly dependent on the catalyst loading amount up to some point, and therefore, increasing the catalyst loading amount may be one of the methods for the improvement of the cell performance. In this study, the increase in the catalyst loading amount at the cathode which occupies most of the electrode overpotential has been tried. Figure 7 shows the effect of the catalyst loading amount at the cathode on the cell performance for the different oxidants of oxygen and air. It is seen that the increase in the cell performance was not significant although the loading amount increased 1.75 times from 0.4 to 0.7 mg/cm². This was because the increase in the loading amount made the catalytic layer thicker, which resulted in the increase of the mass transfer resistance. For the better output power, however, the catalyst loading amount at the cathode of the stack was chosen at 0.7 mg/cm², even though the effect was not so significant.

The pressure drop in the stack is one of the important factors for the system integration, because it determines the amount of the required utility power for the gas supply. The gas flow rate and the gas channel pattern give rise to the pressure drop, but for any cases the lower the pressure drop is, the more the system efficiency is. Figure 8 represents the pressures measured at the cathode inlet and outlet of the 100-cell stack along with the cathode flow rates during the blank run without any electrochemical reactions, as well as the pressure drop through the cathode channel. For the cathode side ΔP was about 0.1 atm at an oxygen flow rate of 800 *l*/min. However, the pressure drop at the anode side was measured zero. No pressure drop at the anode side was due to the fact that the viscosity of hydrogen was quite lower than that of oxygen[12]. Therefore, it was seen that the channel type and the channel dimension adopted in this study did not generate any significant pressure drop at the given operating conditions. During the real operation under load, however, the slight increase in the pressure drop

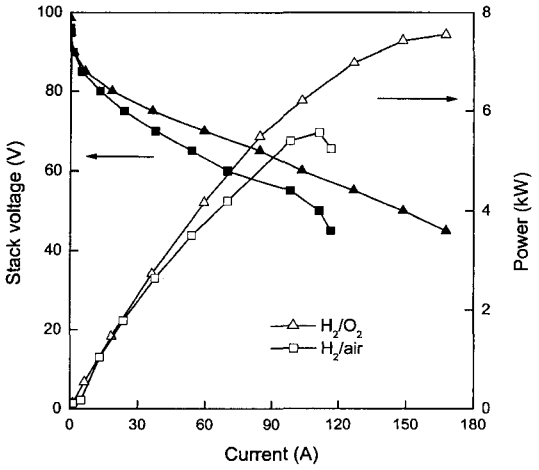

Fig. 9. Performance of the 100-cell stack for H_2/O_2 and H_2/air.

at the cathode side is expected due to the increased pressure at the cathode outlet, which stemmed from the water produced from the electrochemical reaction.

Figure 9 shows the performance of the 100-cell stack, which was operated using H_2 and O_2 at a fuel utilization of 0.5 and an oxidant utilization of 0.25. These utilization were based on the current density of 431 mA/cm^2. The performance of the stack was measured after it was kept moisturized with humidified N_2 for 24 hrs at 70°C. As can be seen in the figure, open circuit voltage (OCV) of the stack is 100 V, with the average OCV of each unit cell being 1.00 V. The OCV value of the stack is lower by about 230 mV than that of the theoretical value calculated from Nernst equation. The discrepancy between the actual and theoretical OCV values, as is well known, is mainly caused by activation polarization of the PEMFC, which is operated at a relatively low temperature. In addition, the low purity of the water, which is used for the humidification of the polymer electrolyte membrane, may provide another reason for the loss in current. The average OCV of the unit cells in the stack is also lower than that of the 25 cm^2 single cell by 20 mV. It seems that there is a minute cross-over through some membranes in the stack. But it did not cause any further problems in operating the stack during the further operation. The stack shows the current of 103.5 A (431 mA/cm^2) at 60 V (0.6 V/cell), and thus 6.21 kW (0.26 W/cm^2/cell) in output power. The maximum electric power obtained under the given conditions was 148.8 A (620 mA/cm^2) at 50 V (0.5 V/cell), i.e., 7.44 kW (0.31 W/cm^2/cell).

The effect of oxidants on the i-V characteristics and the powers is also shown in Fig. 9. At the stack voltage of 60 V (0.6 V/cell), the stack current for oxygen and air was 103.5 A (6.21 kW) and 70 A (4.2 kW), respectively. Therefore, it was seen that the performance of the stack decreased by 32.4% when oxidant was changed from oxygen to air. At 50 V (0.5 V/cell), the stack current for oxygen and air was 148.8 A (7.44 kW) and 111.2 A (5.56 kW), respectively. The oxygen gain increases with an increase in load in general, because the slops of i-V curves in Fig. 9 are not the same for oxygen and air. However, the oxygen gain at the higher current density region was more significant than expected. Also, the maximum

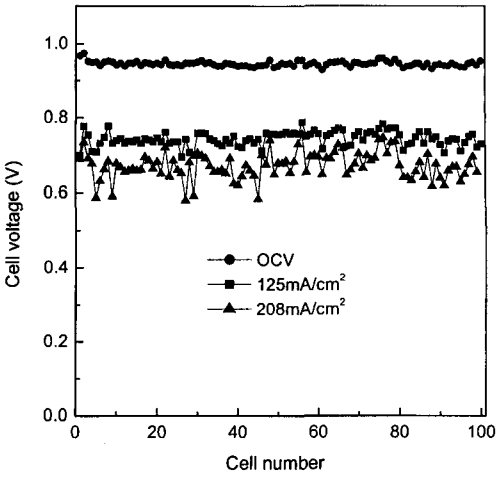

Fig. 10. Distribution of the cell voltage in the stack.

power of the stack was about 20~25% lower than the designed value. The reason for all these phenomena is thought to be non-uniformity of the unit cells in the stack caused during assembling, as discussed below.

Figure 10 shows the voltage distribution of unit cells in the stack. The nearest cell to the cathode gas inlet was assigned No. 1 cell. The distribution of the OCV for unit cells was uniform but the voltage deviation increased as the load increased. Particularly, the voltages of the 5th, 9th, 27th, 29th and 45th cell at the load of 208 mA/cm^2 were lower than those of the other cells. It seems that the electrode polarization for those cells might be influenced by some problems occurred during electrode preparation, stacking, or operation. The average voltage loss, namely the difference between OCV and the voltage at 208 mA/cm^2, is about 0.3 V, and such loss is composed of several elements. The first one is the Nernst loss, which is the difference between OCV and the voltage at a current density of zero, obtained by extrapolating the i-V curve. Although the Nernst loss varies with fuel utilization, the Nernst loss of the stack in this study where pure H_2 and O_2 were used appeared very small. It is likely that the voltage loss mainly resulted from the IR drop and the electrode polarization.

A 5-passenger golf cart was modified to accommodate the stack and the relevant equipment. The vehicle consisted of 100-cell stack, stack operating apparatus, PLC-controller, DC/DC converter, auxiliary

Fig. 11. Photograph of the fuel cell/battery hybrid golf cart.

power source of batteries (48 V, 60 Ah), and gas cylinders stored in the cabinet. For the stack humidification, the nozzle-type humidifiers were adopted instead of the bubbler or membrane humidifier, to save the humidification volume. The humidities at the anode and cathode inlet were monitored to be almost 100% at room temperature. The flow rates of hydrogen and oxygen were set at 30 *l*/min, respectively, with U_f= 0.75 and U_o=0.37 but the hydrogen exhaust was burned out at the anode exit for simplicity, instead of being recirculated. Figure 11 represents the photograph of the fuel cell/battery hybrid golf cart with the 100-cell stack and Table 1 summarizes the specification. When starting the vehicle was designed to be driven by batteries only, but during the normal driving condition the fuel cell would be the main power source, with the batteries being the auxiliary power, if needed. When the vehicle stops the battery would be recharged by the fuel cell. Two 10 *l* aluminum cylinders, one each for hydrogen and oxygen, were equipped for 2 hour-driving at a speed of 20 km/hr. The test drive has been successfully carried out with all components functioning well.

Figure 12 shows the voltage and current variation of the fuel cell during the vehicle operation for 20 min. When the vehicle stopped during the period of 0~2, 6~7, 11~12, and 16.5~19 minutes, the batteries were recharged from the fuel cell stack of which voltage and current were 82 V and 6 A, respectively. During the vehicle driving at 3.5~5, 10~11, 13.5~16.5 minutes, the fuel cell stack produced 20 A at 50 V, namely about 1 kW. This output power occupied about 43% of the total power required by the 2.3 kW motor; while the remaining necessary powers were supplied by the batteries. The stack was originally designed to supply all the power necessary for the motor, but the stack temperature was maintained at around room temperature as the current was not high enough and therefore the stack could not produce full powers. High temperature operation, gas flow rate control according to the load variation, hydrogen exhaust recirculation, methanol reformer for the hydrogen source, air blower instead of the oxygen cylinder,

Table 1. Specification of the fuel cell/battery hybrid golf cart.

Term		Specification
Dimension	L×W×H (cm)	314×120×124
	Number of Passengers	2
Performance	Max. Speed (km/hr)	20
	Range (km)	40
Fuel cell	Max. Power (kW)	7.44
	Number of cells	100
	L×W×H (cm)	80×40×25
Gas cylinder (H_2, O_2)	Storage capacity (m^3)	2 (25°C, 1 atm)
	D×H (cm)	12×100
	Volume (*l*)	10 (2 ea)
Motor	Type	DC motor
	Max. Power (kW)	2.3
Auxiliary power source	Type	Lead acid battery
	Capacity	48 V, 60 Ah

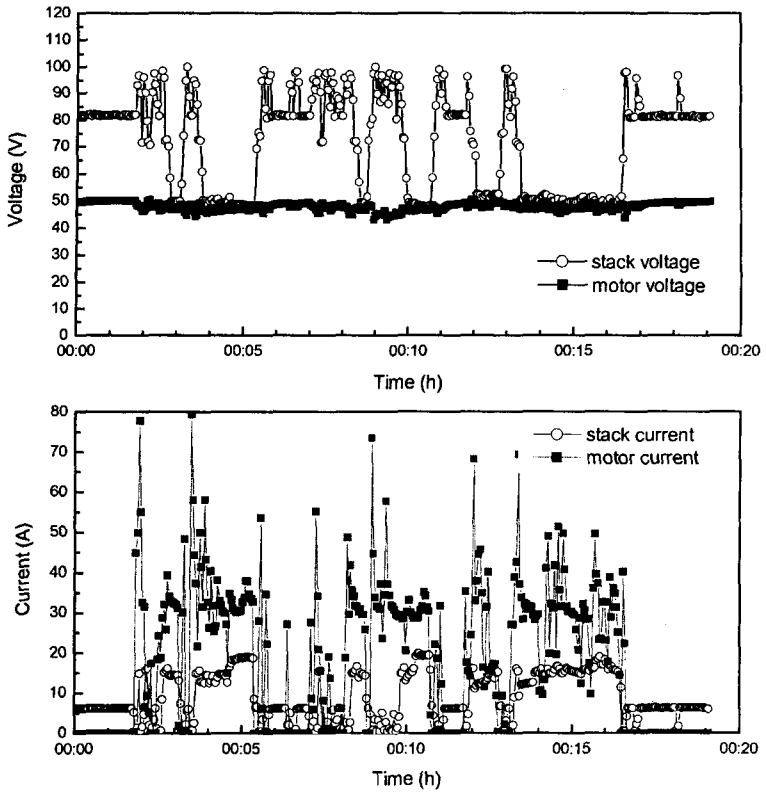

Fig. 12. Variation of the voltage and current for the fuel cell stack and motor during FCV driving.

and so on will be the next tasks for the upgrade of the current fuel cell vehicle.

4. Conclusions

To fabricate the multi-kW class PEMFC stack with a large size electrode, the size effect of the electrode area on the cell performance was first investigated. It was shown that as the electrode area increased from 25 to 240 cm^2, the cell performance decreased from 0.56 W/cm^2 to 0.3 W/cm^2 at 0.6 V due to the scale up problems. Therefore, the single cell with an electrode area of 240 cm^2 could produce a maximum power of 100 W for oxygen and 70 W for air. A counter-flow type 100-cell stack was fabricated using the 240 cm^2 electrodes with a Pt loading amount of 0.4 and 0.7 mg/cm^2 for anode and cathode, respectively. A blank run showed that the pressure drop at the cathode side was about 0.1 atm at an oxygen flow rate of 800 *l*/min and that at the anode side was measured zero, revealing that the flow field pattern and the flow channel dimension adopted in this study did not generate any significant pressure drop at the given operating conditions. The stack at the operating conditions of 70°C and 1 atm showed a maximum power of 7.44 kW (0.31 W/cm^2/cell) for H_2/O_2 and 5.56 kW (0.23 W/cm^2/cell) for H_2/air. The maximum power of the stack was about 20~25% lower than the designed output power of the stack, namely 10 kW for oxygen and 7 kW for air, which was caused by non-uniformity of the unit cells in the stack due to the IR drop and the electrode polarization.

The stack was applied to the power source of the fuel cell/battery hybrid electric golf cart, which was composed of the 100-cell stack, nozzle-type humidifiers, stack operating apparatus, PLC-controller, DC/DC converter, auxiliary power source of batteries (48 V, 60 Ah), and gas cylinders. Two 10 *l* aluminum cylinders, one each for hydrogen and oxygen, were equipped for 2 hour-driving at a speed of 20 km/hr. The voltage

and current variation of the fuel cell stack during the vehicle operation showed that the batteries were recharged from the fuel cell stack during the idle operation and the fuel cell stack produced 20 A at 50 V, namely about 1kW, during the normal driving. This output power occupied about 43% of the total power required by the 2.3 kW motor; while the remaining necessary powers were supplied by the batteries. The stack was originally designed to supply all the power necessary for the motor. However, the stack temperature was maintained at around room temperature as the current was not high enough and, therefore, the stack could not produce full powers.

References

1. Blomen, L.J.M.J. and Mugerwa, M.N.: "Fuel Cell Systems", Plenum Press, New York (1993).
2. Kordesch, K. and Simader, G.: "Fuel Cells and Their Applications", VCH, Weinheim, Germany (1996).
3. Oh, I.-H. and Hong, S.-A.: Korea Energy Forum Bulletin, 59, 22 (2002).
4. Oh, I.-H., Choi, H.-J., Ahn, S.-Y., Ha, H.Y., Shim, J.-P., Cha, S.-Y., Hong, S.A. and Lim, T.W.: Proceedings of the 3rd International Fuel Cell Conference, Nagoya, November 30-December 3, 567 (1999).
5. Lee, J.-K., Ha, H.Y., Hong, S.-A., Chun, H.-S., Lim, T.W. and Oh, I.-H.: Hwahak Konghak, 39(1), 109 (2001).
6. Shin, S.-J., Lee, J.-K., Ha, H.Y., Hong, S.A., Chun, H.-S. and Oh, I.-H.: J. of Power Sources, 106, 146 (2002).
7. Ahn, S.Y., Shin, S.-J., Ha, H.Y., Hong, S.-A., Lee, Y.-C., Lim, T.W. and Oh, I.-H.: J. of Power Sources, 106, 295 (2002).
8. Shim, J., Ha, H.Y., Hong, S.-A. and Oh, I.-H.: J. of Power Sources, 109, 412 (2002).
9. Oh, I.-H., Ha, H.Y., Jo, J.-H., Ahn, S.-Y., Cho, S.-A. and Hong, S.-A.: Proceeding of the 8th Next Generation Vehicle Workshop, Cheonan, September, 6-7, 600 (2000).
10. Oh, I.-H., Ahn, S.-Y., Jo, J.-H., Lee, J.-K., Ha, H.Y., Hong, S.-A. and Lim, T.W.: Proceeding of the 2000 Fuel Cell Seminar, Portland, October 30-November 2, 428 (2000).
11. Srinivasan, S., Ticianelli, E.A., Derouin, C.R. and Redondo, A.: J. Power Sources, 22, 359 (1988).
12. Bird, R.B., Stewart, W.E. and Lightfoot, E.N.: "Transport Phenomena", John Wiley & Sons, Inc., New York (1960).